R. & M. No. 3567

R. & M. No. 3567

MINISTRY OF TECHNOLOGY

AERONAUTICAL RESEARCH COUNCIL
REPORTS AND MEMORANDA

A General Method of Studying Steady Lift Interference in Slotted and Perforated Tunnels

By K. R. Rushton and Lucy M. Laing

LIBRARY
ROYAL AIR[illegible]
BEDFORD.

LONDON: HER MAJESTY'S STATIONERY OFFICE
1969
PRICE 13*s.* 0*d.* NET

A General Method of Studying Steady Lift Interference in Slotted and Perforated Tunnels

By K. R. Rushton and Lucy M. Laing

Department of Civil Engineering, University of Birmingham

Reports and Memoranda No. 3567*
February, 1967

Summary.

A study of steady lift interference effects in wind tunnels with several different wall conditions has been carried out using a three-dimensional resistance network. The methods by which the various boundary conditions were simulated on the network are described in detail; conditions included closed, open, slotted and perforated walls. The evaluation of interference parameters is described, and for a completely closed tunnel these parameters are compared with analytical results. Numerous other examples of a rectangular wind tunnel have been studied and the resultant interference parameters are tabulated.

CONTENTS

Section

1. Introduction

2. Mathematical Background
   - 2.1. Governing equation
   - 2.2. The small wing
   - 2.3. Boundary conditions
   - 2.4. Interference parameters

3. Finite Difference Solution using Resistance Network
   - 3.1. Resistance network analogue to the finite difference equations
   - 3.2. Choice of mesh spacing
   - 3.3. Simulation of the wing
   - 3.4. Boundary conditions

4. The Closed Square Tunnel

*Replaces A.R.C. 29 237.

CONTENTS—*continued*

Section

5. Different Tunnel Configurations

5.1. Streamline curvature corrections in ideal slotted tunnel with solid side walls

5.2. Perforated tunnel

5.3. A typical tunnel

5.4. Slots covered with perforations

6. Conclusions

7. Acknowledgements

List of Symbols

References

Appendix

Illustrations—Figs. 1 to 14

Detachable Abstract Cards

---

1. *Introduction.*

Due to the presence of the walls of a wind tunnel, the flow around a wing is different from that in an infinite field. This difference between the two states of flow is termed the interference. One particular form of interference will be discussed in this Report, namely the lift interference.

A reduction in the magnitude of this interference can result from certain modifications to the tunnel walls; typical modifications are the introduction of longitudinal slots or perforations. Therefore, consideration has been given to developing a general method of studying lift interference on small wings in slotted and perforated tunnels.

The lift interference in a wind tunnel can be analysed by determining the distribution of the perturbation velocity potential throughout the tunnel. If the analysis is restricted to linearised compressible flow, the distribution of the perturbation velocity potential is governed by the Laplace equation in three dimensions. Any particular problem can then be analysed by modelling the small lifting wing at the centre of the tunnel with boundary conditions set on the tunnel walls to simulate the type of wall under consideration. The following wall conditions commonly occur; closed and open walls, ideal slotted walls, perforated walls and slotted walls with viscous effects.

In an earlier report[1] ideal slotted wall interference effects in the wake of an oscillating wing were studied by an electrical analogue of a linear partial differential equation in two dimensions. The basis of the analogue is that the network of resistances has the same equations as the finite difference form of the governing equation. From this previous study, information concerning the steady upwash interference in the plane of the wing for slotted-wall tunnels was obtained from the two dimensional solution. But further information concerning the streamline curvature, or streamwise gradient of interference upwash, needs a three-dimensional solution on the resistance network. A three-dimensional network also permits the representation of perforated and non-ideal slotted boundaries. While the method of representing ideal slotted boundaries is the same as for the two-dimensional analysis, the perforated and non-ideal slotted boundaries require more complicated techniques involving a step by step method.

The first part of this Report describes the resistance analogue and the techniques required to represent the various boundary conditions. Then the closed tunnel is considered in detail and the accuracy of the network method is assessed by comparing the analogue results for the closed tunnel with certain analytical results. This is followed by a detailed examination of square tunnels with various wall conditions.

2. *Mathematical Background.*

2.1. *Governing Equation.*

The governing equation for linearised compressible flow of Mach number M is,

$$(1-M^2)\frac{\partial^2\phi}{\partial x^2}+\frac{\partial^2\phi}{\partial y^2}+\frac{\partial^2\phi}{\partial z^2}=\frac{M^2}{U^2}\left(\frac{\partial^2\phi}{\partial t^2}+2U\frac{\partial^2\phi}{\partial x\partial t}\right) \tag{1}$$

where ϕ is the perturbation velocity potential and x, y, z are the Cartesian co-ordinates, Figure 1. For steady flow the equation reduces to

$$(1-M^2)\frac{\partial^2\phi}{\partial x^2}+\frac{\partial^2\phi}{\partial y^2}+\frac{\partial^2\phi}{\partial z^2}=0 \tag{2}$$

By the transformation

$$x=\tfrac{1}{2}\beta hX\,,\ y=\tfrac{1}{2}hY\,,\ z=\tfrac{1}{2}hZ \tag{3}$$

where $\beta=(1-M^2)^{\frac{1}{2}}$ and h is the height of the tunnel, equation (2) reduces to the Laplace equation

$$\frac{\partial^2\phi}{\partial X^2}+\frac{\partial^2\phi}{\partial Y^2}+\frac{\partial^2\phi}{\partial Z^2}=0 \tag{4}$$

In the following analysis the interference effects are measured by the difference between the perturbation velocity potential within the tunnel, ϕ, and for the same model in a field of infinite extent, ϕ_m. The difference between these two quantities is called interference velocity potential.

$$\phi_i=\phi-\phi_m. \tag{5}$$

Since both ϕ and ϕ_m satisfy the Laplace equation, ϕ_i also satisfies the Laplace equation.

The results are to be presented in terms of the interference upwash velocity $\partial\phi_i/\partial z$ and the streamline curvature which is proportional to $\partial^2\phi_i/\partial x\partial z$, and therefore the interference potential must be determined to a good accuracy. Moreover the interference potential is often far smaller than ϕ and ϕ_m, and cannot be obtained to a sufficient accuracy by solving for these and taking the difference $\phi-\phi_m$.

Thus an alternative method is adopted whereby the accurate values of ϕ_i are obtained from two successive solutions of the Laplace equation. The first analysis is in terms of ϕ, and from this solution and a knowledge of the values of ϕ_m on the boundary, the boundary values of ϕ_i can be calculated from equation (5). These values of ϕ_i are then set as boundary conditions for a second solution of the Laplace equation. The boundary conditions applied in both solutions are shown in Figure 6. The accuracy of this method was discussed in Reference (1).

In practice two iterations, i.e. four solutions, have to be obtained, because of initial approximations in representing the small lifting wing, (*see* Section 2.2). Initially the value of ϕ on the small arc surrounding the wing is set equal to the value of ϕ_m at these points. Once an approximate distribution of ϕ_i has been obtained for an analysis in terms of ϕ_i, then a more accurate value of $\phi=\phi_m+\phi_i$ can be set around the wing.

In this study only rectangular tunnels are considered having a height h and breadth b. Ideally the tunnel should extend from minus infinity to plus infinity, but when obtaining a solution using a finite difference method it is impractical to represent infinity. Therefore a finite length of tunnel, $-8 \leqslant X \leqslant 8$, was considered. On the upstream and downstream boundaries, the boundary condition to be enforced is $\partial\phi/\partial X = 0$. The adequacy of this assumption is discussed with reference to a particular example, Section 5.

2.2. *The Small Wing.*

A small wing is positioned at the origin of the tunnel, Figure 1. It is represented as a vortex doublet starting at the wing tip and extending infinitely far downstream. The perturbation velocity potential of this vortex pair can be expressed as,

$$\phi_m = \frac{USC_L z}{8\pi(y^2+z^2)}\left(1+\frac{x}{(x^2+\beta^2 y^2+\beta^2 z^2)^{\frac{1}{2}}}\right) \tag{6}$$

In terms of the co-ordinates X, Y and Z,

$$\phi_m = \frac{USC_L Z}{4\pi h(Y^2+Z^2)}\left(1+\frac{X}{(X^2+Y^2+Z^2)^{\frac{1}{2}}}\right) \tag{7}$$

Equation (7) indicates that in the wake of the small wing ($X \geqslant 0$, $Y = Z = 0$), ϕ takes an infinite value. This cannot be satisfied directly with a finite difference method, and therefore values of ϕ_m are calculated for a small arc surrounding the wing, and are set on the equivalent nodes of the resistance network. Figure 2 indicates the shape of the arc on which the potentials are set.

2.3. *Boundary Conditions.*

A variety of boundary conditions occur on the walls of wind tunnels; they are each described below, and are then formulated in mathematical terms for rectangular tunnels.

(i) *The open boundary.* On the open, or free, boundary, the pressure remains constant and equals the undisturbed pressure far upstream. The assumption is made that this condition may be linearized and applied as if the free boundaries are not distorted by the presence of the wing. Thus the perturbation velocity potential is zero, i.e.

$$\phi = 0. \tag{8}$$

(ii) *The closed boundary.* On a closed wall there is no velocity component normal to the wall; thus

$$\partial\phi/\partial n = 0 \tag{9}$$

where n is the outward direction normal to the wall. Hence for a rectangular tunnel the conditions on the side walls are that $\partial\phi/\partial Y = 0$ and on the roof and floor $\partial\phi/\partial Z = 0$.

(iii) *The ideal slotted boundary.* For an ideal slotted wall, as an alternative to applying separate conditions for the slots and slats, an equivalent homogeneous condition,[2]

$$\partial\phi/\partial x + K\partial^2\phi/\partial x\partial n = 0, \tag{10}$$

is often used. This can be integrated to give

$$\phi \pm K\,\partial\phi/\partial y = 0 \text{ on the side wall } y = \pm\tfrac{1}{2}b$$

and

$$\phi \pm K\,\partial\phi/\partial z = 0 \text{ on the roof or floor of the tunnel.}$$

Previous studies using the resistance network[1] have indicated that for four or more slots the homogeneous condition is a good approximation.

By the transformations of equation (3), the homogeneous conditions become

$$\phi + F\,\partial\phi/\partial|Y| = 0$$
$$\phi + F\,\partial\phi/\partial|Z| = 0 \quad , \tag{11}$$

where $F = 2K/h$ is a non-dimensional slot parameter.

(iv) *The perforated boundary.* Perforated wind-tunnel walls have a large number of usually circular openings, and it is assumed that the outflow and pressure drop across the boundary are proportional. A linearised approximation leads to the equation,

$$\frac{\partial\phi}{\partial x} + \frac{1}{P}\frac{\partial\phi}{\partial n} = 0 \tag{12}$$

where P is the porosity parameter. The transformation of equation (3) leads to the conditions

$$\partial\phi/\partial X + (\beta/P)\,\partial\phi/\partial|Y| = 0 \text{ on } |Y| = b/h$$
$$\partial\phi/\partial X + (\beta/P)\,\partial\phi/\partial|Z| = 0 \text{ on } |Z| = 1 \tag{13}$$

(v) *The non-ideal slotted boundaries.* If a slotted tunnel wall has viscous effects within the slots, the homogeneous conditions for ideal slotted and perforated boundaries can be combined to give[3]

$$\partial\phi/\partial X + F\,\partial^2\phi/\partial X\partial|Y| + (\beta/P)\,\partial\phi/\partial|Y| = 0$$
$$\partial\phi/\partial X + F\,\partial^2\phi/\partial X\partial|Z| + (\beta/P)\,\partial\phi/\partial|Z| = 0 \tag{14}$$

2.4. *Interference Parameters.*

The interference effects in rectangular tunnels are expressed approximately in terms of the following four parameters.

(i) The local interference upwash, δ_0, at a small wing is defined by

$$\delta_0 = \frac{2b}{USC_L}\left(\frac{\partial\phi_i}{\partial Z}\right)_0, \tag{15}$$

where $(\partial\phi_i/\partial Z)_0$ at the origin is evaluated from the analogue solution by numerical differentiation using a three-point finite-difference formula.

(ii) The distribution of the interference upwash along the axis of the tunnel, δ, is expressed as,

$$\delta = \delta(X) = \frac{2b}{USC_L}\left(\frac{\partial\phi_i}{\delta Z}\right), \tag{16}$$

where $(\partial\phi_i/\partial Z)$ is evaluated on the axis of the tunnel $Y = Z = 0$.

(iii) The third parameter, δ_0' is defined by

$$\delta_0' = -\frac{1}{h}\int_{-\infty}^{0} \delta(X)\,dX, \tag{17}$$

where $\delta(X)$ is defined in equation (16).

The evaluation of this parameter is considered in the Appendix.

(iv) The final parameter, δ_1, denotes the steady streamline curvature,

$$\delta_1 = \frac{4b}{USC_L}\left(\frac{\partial^2\phi_i}{\partial X\partial Z}\right)_0 \tag{18}$$

The quantity $(\partial^2\phi_i/\partial X\partial Z)$ is evaluated at the origin using a finite-difference expression.

Generally wind tunnels of any shape are expressed approximately in terms of three parameters δ_0, δ_0' and δ_1.

3. *Finite-Difference Solution using Resistance Network.*

General analytical solutions to the type of problem specified in the previous Section are not available, but solutions can be obtained by the numerical technique of finite differences. This technique requires that the governing equation and the boundary conditions are expressed in finite-difference form resulting in a large number of simultaneous equations. The solution of these equations for a three-dimensional field can either be obtained with a digital computer or by means of a pure resistance analogue computer. Since a large number of solutions is required for each tunnel shape, the analogue computer method is selected.

The analogue computer has been used previously to investigate two-dimensional problems of slotted-wall interference, and its extension to represent three-dimensional problems requires a more complex resistance network together with additional techniques to represent the boundaries. Since the analogue computer solves instantaneously the finite-difference equations, the convergence of any iterative techniques required on the boundaries can be traced.

3.1. *Resistance Network Analogue to the Finite Difference Equations.*

The Laplace equation,

$$\partial^2\phi/\partial X^2+\partial^2\phi/\partial Y^2+\partial^2\phi/\partial Z^2 = 0 \tag{4}$$

can now be written in finite difference form for the irregular Cartesian mesh shown in Figure 3a as follows:

$$\frac{\partial^2\phi}{\partial X^2}+\frac{\partial^2\phi}{\partial Y^2}+\frac{\partial^2\phi}{\partial Z^2} = \frac{2}{d_1+d_3}\left(\frac{\phi_1-\phi_0}{d_1}+\frac{\phi_3-\phi_0}{d_3}\right) \tag{19}$$

$$+\frac{2}{d_2+d_4}\left(\frac{\phi_2-\phi_0}{d_2}+\frac{\phi_4-\phi_0}{d_4}\right)+\frac{2}{d_5+d_6}\left(\frac{\phi_5-\phi_0}{d_5}+\frac{\phi_6-\phi_0}{d_6}\right) = 0$$

If a resistance network is constructed by inserting resistances between terminals corresponding to the nodes of the finite-difference net, Figure 3b, then the condition that the total current entering node, 0, is zero leads to the equation,

$$\frac{V_1-V_0}{R_1}+\frac{V_2-V_0}{R_2}+\frac{V_3-V_0}{R_3}+\frac{V_4-V_0}{R_4}+\frac{V_5-V_0}{R_5}+\frac{V_6-V_0}{R_6} = 0 \tag{20}$$

For this electrical equation to be analogous to the finite-difference equation, each resistance must be chosen so that it is proportional to the mesh spacing and inversely proportional to the cross section that it represents, Figure 3c. For example,

$$\begin{aligned} R_1 &= G\left[4d_1/(d_2+d_4)(d_5+d_6)\right] \\ R_5 &= G\left[4d_5/(d_1+d_3)(d_2+d_4)\right] \end{aligned} \tag{21}$$

where G is a scaling factor chosen to give resistances of suitable magnitude.

If a similar method of derivation is followed for any other node, identical magnitudes are obtained for each resistor when considering the condition of zero total current for nodes at either end of a resistor.

When these resistance values are substituted in equation (20) and the whole equation is multiplied through by a constant proportional to the volume represented by the node 0, $8G/(d_1+d_3)\ (d_2+d_4)\ (d_5+d_6)$, then the resultant equation,

$$\frac{2}{d_1+d_3}\left(\frac{V_1-V_0}{d_1}+\frac{V_3-V_0}{d_3}\right)+\frac{2}{d_2+d_4}\left(\frac{V_2-V_0}{d_2}+\frac{V_4-V_0}{d_4}\right)$$
$$+\frac{2}{d_5+d_6}\left(\frac{V_5-V_0}{d_5}+\frac{V_6-V_0}{d_6}\right)=0 \tag{22}$$

is analogous to the finite-difference equation (19). Hence the velocity potential and the electrical potential are analogous quantities, thus

$$V = G'\phi \tag{23}$$

where G' is a suitable scaling factor.

This single network can be used both for solutions in ϕ and in ϕ_i, since both satisfy the Laplace equation and refer to the same size of field.

3.2. *Choice of Mesh Spacing.*

For the particular problem of the three-dimensional wind tunnel the mesh is designed to model a field with the breadth approximately equal to the height, extending a distance of four times the height upstream and downstream of the point wing. Ideally a uniform mesh spacing should be provided through the field to minimise the truncation error, but this is uneconomical in the cost of the equipment, and therefore graded nets are adopted. Not only must the mesh be designed to cover the entire field, but also the mesh spacing on each cross section must be arranged to provide a fine mesh around the point wing with a gradual increase in mesh interval towards the boundary.

On a plane X = constant the smallest mesh interval is taken to be $h/32$, with the largest interval of $h/8$. Figure 4a illustrates the mesh spacing for a plane X = constant; in particular the method of continuing all mesh lines through to the boundary should be noted. Due to symmetry only one quarter of the tunnel need be modelled, with symmetry about the plane $Z = 0$, and antisymmetry about the plane $Y = 0$.

A similar form of grading is adopted along the length of the tunnel. In the neighbourhood of the point wing the minimum mesh spacing is $\beta h/32$, whereas, towards the ends of the tunnel, the mesh spacing is increased to $2\beta h$. This spacing is arranged so that there is a close mesh spacing in regions where a rapid change in distribution of ϕ occurs, whilst a wider spacing is used in regions with a slow change in the function, the spacing is indicated in Figure 7.

3.3. *Simulation of the Wing.*

The point wing is represented on each cross section by applying to nodes surrounding the axis $Y = Z = 0$, voltages equivalent to the values of ϕ_m at those points. Figure 2 indicates the nodes to which the potentials are applied to an accuracy of $\pm 0{\cdot}01$ per cent of the maximum potential. After this initial experiment a second experiment is performed in terms of ϕ_i. An improved representation of the wing can then be achieved by applying equivalent to $\phi_m+\phi_i$ to the nodes surrounding the axis.

3.4. *Boundary Conditions.*

Of the five types of boundary condition listed in Section 2.3, four involve the normal slope $\partial\phi/\partial n$. Therefore consideration will be given first to the method of setting a specified slope; then the method of representing each of the boundary conditions will be considered in turn.

Take a typical node 0 positioned on the boundary Z = constant where the condition to be satisfied is that $(\partial\phi/\partial Z)_0$ is specified. Reference to Figure 5 indicates that a fictitious node, 5, occurs, which is positioned at a distance d_6 from node 0. The function at node 5 can be replaced by the expression,

$$\phi_5 = \phi_6 + 2d_6\,(\partial\phi/\partial Z)_0\,.$$

The Laplace equation at node 0 then becomes

$$\frac{\partial^2\phi}{\partial X^2}+\frac{\partial^2\phi}{\partial Y^2}+\frac{\partial^2\phi}{\partial Z^2} = \frac{2}{d_1+d_3}\left(\frac{\phi_1-\phi_0}{d_1}+\frac{\phi_3-\phi_0}{d_3}\right) \tag{24}$$

$$+\frac{2}{d_2+d_4}\left(\frac{\phi_2-\phi_0}{d_2}+\frac{\phi_4-\phi_0}{d_4}\right)+\frac{2}{d_6}\left(\frac{\phi_6-\phi_0}{d_6}\right)+\frac{2}{d_6}\left(\frac{\partial\phi}{\partial Z}\right)_0 = 0$$

If on the resistance network the resistor R_5 is replaced by an alternative resistor R' with a voltage U_0 applied at its end, then

$$\frac{V_1-V_0}{R_1}+\frac{V_2-V_0}{R_2}+\frac{V_3-V_0}{R_3}+\frac{V_4-V_0}{R_4}+\frac{V_6-V_0}{R_6}+\frac{U_0-V_0}{R'} = 0 \tag{25}$$

The resistors are chosen in the same manner as before to represent the real part of the tunnel; for example,

$$R_1 = G\,[4d_1/(d_2+d_4)\,d_6]$$

and

$$R_6 = G\,[4d_6/(d_1+d_3)\,(d_2+d_4)]\,.$$

On substituting for these values and multiplying through by the term proportional to the volume, $8G/(d_1+d_3)\,(d_2+d_4)\,d_6$, the following equation is obtained:

$$\frac{2}{d_1+d_3}\left(\frac{V_1-V_0}{d_1}+\frac{V_3-V_0}{d_3}\right)+\frac{2}{d_2+d_4}\left(\frac{V_2-V_0}{d_2}+\frac{V_4-V_0}{d_4}\right)$$

$$+\frac{2}{d_6}\left(\frac{V_6-V_0}{d_6}\right)+\frac{8G}{(d_1+d_3)\,(d_2+d_4)\,d_6}\,\frac{U_0-V_0}{R'} = 0 \tag{26}$$

Equations (24) and (26) are of similar form, and since $V = G'\phi$, the final terms of the expression can be equated to give,

$$\frac{U_0-V_0}{R'} = \frac{(d_1+d_3)\,(d_2+d_4)}{4}\,\frac{G'}{G}\left(\frac{\partial\phi}{\partial Z}\right)_0 \tag{27}$$

A similar expression can be derived when $(\partial\phi/\partial Y)$ is specified on a boundary Y = constant.

If the resistance R' is selected so that U_0 is very much greater than V_0, then during the initial setting of the network the voltage U_0 can be applied to be proportional to $(\partial\phi/\partial Z)_0$. Before the final measurements are taken, the voltage U_0 must be readjusted so that $U_0 - V_0$ is proportional to $(\partial\phi/\partial Z)_0$. However the voltage V_0 is generally less than 1 per cent of U_0, and therefore the readjustment is trivial.

(i) *The open boundary.* On the open boundary the condition that the perturbation velocity potential is zero can be applied to the network directly by setting zero voltage on the nodes at the boundary.

(ii) *The closed boundary.* A closed boundary on the plane Z = constant is described by the condition $\partial\phi/\partial Z = 0$. Reference to equation (27) indicates that this condition can be satisfied automatically by

omitting the boundary resistors, R, and leaving the boundary nodes free to take their own voltage.

(iii) *The ideal slotted boundary.* If the equivalent homogeneous condition is to be satisfied on the tunnel roof, then

$$\phi_0 + F(\partial\phi/\partial Z)_0 = 0$$

or

$$(\partial\phi/\partial Z)_0 = -\phi_0/F = -V_0/FG'$$

With this substitution equation (27) becomes,

$$(U_0 - V_0)/R' = -(d_1 + d_3)(d_2 + d_4)\, V_0/4GF \tag{28}$$

Now if the resistance R' is selected so that

$$1/R' = (d_1 + d_3)(d_2 + d_4)/4GF\,, \tag{29}$$

then this condition will be satisfied by setting the voltage $U_0 = 0$.

Therefore the homogeneous condition can be satisfied on the tunnel roof by connecting to every boundary node a resistance calculated according to equation (29) and applying zero potential to the other end of these resistances. An identical method is adopted to satisfy the homogeneous condition on the side wall $Y = b/h$.

(iv) *The perforated boundary.* The perforated boundary, unlike those described previously, cannot be represented automatically on the resistance network, but requires an iterative method. By writing the boundary equations for the roof $Z = 1$ as

$$\partial\phi/\partial Z = -(P/\beta)\,\partial\phi/\partial X\,, \tag{30}$$

it becomes apparent that a step by step method can be devised whereby trial values of $\partial\phi/\partial Z$ are enforced on the boundary by setting the appropriate voltage U_0 to the resistors R' to satisfy equation (27); from the resultant potential distribution $\partial\phi/\partial X$ can be calculated, and the trial values of $\partial\phi/\partial Z$ can be adjusted to satisfy the condition of equation (30) at all the nodes on the boundary. Thus, by iteration a porous boundary can be modelled.

(a) Resistors, R', are connected to each boundary node of value inversely proportional to $(d_1 + d_3)$ $(d_2 + d_4)$. These resistors are chosen to be of high value compared with the network resistors which ensures that the voltage U_0 is of an order higher than the voltage V_0 $(U_0/V_0 > 100)$. Thus in equation (27) V_0 can be neglected and the voltage U_0 is directly proportional to the slope $(\partial\phi/\partial Z)_0$.

(b) Once the trial values of $(\partial\phi/\partial Z)_0$ have been enforced on the boundaries of the network, the distribution of the function ϕ throughout the tunnel is given immediately by the electrical voltages. However, until the boundary conditions have been satisfied, only the potential distribution on the plane $Z = 1$ need be measured, and from these readings the term $(\partial\phi/\partial X)_0$ can be calculated.

(c) The term $(\partial\phi/\partial X)_0$ is calculated from a suitable finite-difference formula. In regions where the mesh spacing is irregular, three-point formulae are devised so that the first term of the truncation error is h^3. For example, to calculate $(\partial\phi/\partial X)_3$ at the node $X = 3/16$ with values of the function ϕ_3, and ϕ_2 at $X = 2/16$, and ϕ_5 at $X = 5/16$, then

$$(\partial\phi/\partial X)_3 = (1/6h)(\phi_5 + 3\phi_3 - 4\phi_2). \tag{31}$$

(d) The boundary condition is satisfied when, at every node on the boundary plane $Z = 1$, $\partial\phi/\partial Z$ applied to the network in the manner described under (a) equals $-(P/\beta)\,\partial\phi/\partial X$.

The convergence of this method is discussed with reference to examples in Section 5.2. An identical method is used for the perforated side walls.

(v) *The non-ideal slotted boundary.* In representing the slotted boundary with viscous effects a technique similar to that described for the perforated boundary is adopted. Since equation (14) can be expressed as

$$\frac{\partial \phi}{\partial Z} = -\frac{P}{\beta}\left(\frac{\partial \phi}{\partial X} + F\frac{\delta^2 \phi}{\partial X \partial Z}\right) \tag{32}$$

on $Z = 1$, trial values of $(\partial\phi/\partial Z)_0$ can be applied to the network as the equivalent voltage U_0; then from the resultant voltage distribution the right hand side of the expression can be calculated from finite difference expressions. The steps to be followed in satisfying this boundary condition on the resistance network are identical to those listed in the previous sub-section, apart from the need to record more voltage readings from which to evaluate the second derivative. Convergence of this technique is discussed in Section 5.3.

4. *The Closed Square Tunnel.*

For the particular problem of a square tunnel with closed boundaries certain analytical results are available, and by comparing the analogue results with the analytical results an assessment can be made of the reliability with which the resistance networks represent three-dimensional tunnels. The analytical results of Ref. 4 are for tunnels of infinite length having all four walls closed and a small wing positioned at the centre of the tunnel.

The tunnel represented on the resistance network extended in the streamwise direction between the limits $X = \pm 8$. On the upstream and downstream boundaries, the condition enforced was $\partial\phi/\partial X = 0$. On the tunnel walls and roof the closed boundaries require that $\partial\phi/\partial Y = 0$ or $\partial\phi/\partial Z = 0$, and these conditions were satisfied as described in Section 3.4. The small wing was modelled by applying potentials to the arc surrounding the wing, and the four separate solutions were obtained as outlined in Section 3.3. The steps required in obtaining the solution are outlined in Figure 6.

From the final solution in ϕ_i, the distribution of ϕ_i throughout the tunnel was recorded. The analytical solution for the interference potentials within the tunnel has not been evaluated, but certain interference parameters are readily calculated to permit the following comparisons.

(a) The distribution of δ along the axis of the tunnel is known from Ref. 4. A comparison with the analogue results, Figure 7, indicates that the finite-difference solution of the resistance network gives satisfactory results without serious discrepancies due to the limitations in the streamwise direction. The analytical and analogue results for δ_0 and δ_1 are compared in Table 1 and an estimate of the expected accuracy is included in the table.

TABLE 1

	Analytical	Analogue	Estimated Accuracy
δ_0	+0·1368	+0·134	±0·005
δ_1	+0·2401	+0·245	±0·01

(b) The distributions of ϕ and ϕ_i in the plane $X = 0$ can be determined from a two-dimensional finite-difference solution on a resistance network as described in Reference 1. Comparison of the three-dimensional solution in the plane $X = 0$ with a two-dimensional solution using 64 x 64 mesh intervals demonstrated that the differences in ϕ were less than 0·5 per cent of the maximum value of ϕ set on the arc around the wing.

(c) Information is also available concerning the perturbation velocity potential at large streamwise distances. Far upstream ϕ should vanish and on the upstream boundary of the resistance network at $X = -8$ its values were zero apart from a very small random error.

In the distant wake the potential distribution should be double that at the wing. When the results on the plane $X = 8$ are compared with accurate values from the two dimensional solution on the fine network, no error greater than $\pm 0{\cdot}2$ per cent of the maximum potential is found to occur. This confirms that the finite analogue is adequate.

From this detailed examination of the closed square tunnel it is apparent that a satisfactory analysis of the interference effects in steady flow in three-dimensional tunnels can be achieved. Nevertheless, when other tunnel boundary conditions are applied further checks are essential.

5. *Different Tunnel Configurations.*

Various problems with different wall conditions have been studied to give information concerning tunnels of practical interest. For each problem the parameters δ_0 and δ_1 are tabulated and diagrams of the distribution of the interference upwash along the axis of the tunnel are included. Reference is also made to any practical difficulties encountered in the satisfaction of the boundary conditions.

5.1. *Streamline Curvature Corrections in Ideal Slotted Tunnel with Solid Side Walls.*

The first study was aimed at checking the validity of an approximate theory for a tunnel with ideal slotted roof and floor and solid side walls. An approximate expression for the variation of the streamline curvature with the slot parameter F has been suggested in Reference 5, and was evaluated for a tunnel with $h/b = 0{\cdot}89$. The reliability of this result is questionable because in the limiting case of the open roof and floor the result is found to differ from the known analytical value. Therefore the problem has been analysed in detail on the resistance network.

With the resistance network representing the rectangular tunnel, three intermediate values of the slot parameter F were investigated with $(1+F)^{-1} = 0{\cdot}35, 0{\cdot}65, 0{\cdot}85$, together with the limiting values 0 and 1 for the closed and open boundaries. Three sets of boundary resistors, R' were required, one for each value of F; for the closed tunnel no resistor is required whilst for the open tunnel the function $\phi = 0$ is set on each of the boundaries. With the ideal slotted boundaries the operation is automatic, but two rounds of experiments in both ϕ and ϕ_i were required.

A list of the values of δ_0 and δ_1 is to be found in Table 2, and the distribution of δ along the tunnel centreline is indicated in Figure 8. In Figure 9 δ_0 and δ_1 are plotted against $(1+F)^{-1}$ and the values of δ_1 are compared with those recorded in Reference 5. It is seen that the error in the solution of Reference 5 increases as $(1+F)^{-1}$ tends to 1. In the analogue solution the estimated accuracy of δ_1 is $\pm 0{\cdot}025$, the reduced accuracy arising because less accurate resistors were used.

TABLE 2

$(1+F)^{-1}$	δ_0	δ_1
0	+0·130	+0·24
0·35	+0·037	+0·13
0·65	−0·045	+0·01
0·85	−0·100	−0·12
1·0	−0·145	−0·22

5.2. *Perforated Tunnel.*

Tunnels are sometimes constructed with all four walls perforated, and therefore a series of experiments was carried out with a range of values of the porosity parameter β/P. The results quoted at the end of this Section refer to a tunnel having a square cross section with equation (12) satisfied on each wall.

Only one set of the boundary resistors R' was required for all the values of β/P, and to these resistors estimated values of the term $\partial\phi/\partial n$ were applied as voltages U_0. Since convergence to the correct boundary condition cannot be achieved automatically, a step by step method has to be adopted. In this step by step method the conditions are first satisfied along the centreline of the roof of the tunnel, and then lines of nodes with X = constant are considered. If a record is kept of each trial, the manner of convergence becomes clear, between ten and twenty-five adjustments being required.

Table 3 records values of δ_0, and δ_1 for a range of values of β/P. These results are also plotted as curves against $(1+\beta/P)^{-1}$ in Figure 11. Included on the plot of δ_0 are values obtained for the circular tunnel with porous boundaries; the similarity between the square and circular tunnels is very marked.

TABLE 3

β/P	δ_0	δ_1
∞	+0·1340	+0·2416
3·0	+0·06621	+0·216
1·0	−0·01996	+0·0964
0·7	−0·05378	+0·06436
0·3	−0·06988	−0·0364
0·17	−0·09697	−0·11236
0	−0·1381	−0·2080

In addition Figure 10 shows the variation of δ along the tunnel for each value of β/P. The estimated accuracy for δ_0 is $\pm$0·01 and for $\delta_1 \pm$0·02. These are based on a comparison of initial results when the boundary conditions were only approximately satisfied, and the final solution when the boundary conditions were satisfied as closely as possible. The differences in δ_0 and δ_1 between these pairs of solutions were noted and used to assess the probable accuracy. Generally the finite length of the tunnel appeared to have little effect on the results, for even if the tunnel length was halved similar results were obtained. However for the smaller values of β/P, the magnitude of the parameter δ varied rapidly downstream from the wing in the region $2 < X < \infty$. Since there is only a coarse net in this region, the accuracy of the results within this region for $\beta/P = 0{\cdot}17$ and 0·30 are only approximate.

5.3. *A Typical Tunnel.*

In a further study the resistance network was used to represent the NPL 25 in. by 20 in. tunnel[6]. The tunnel was assumed to have a square cross section with closed side walls but with the following conditions on the roof and floor.

(1) Ideal slotted tunnel with $F = 0{\cdot}1073$ on the roof.

(2) Non-ideal slotted tunnel with $F = 0{\cdot}1073$ and $\beta/P = 1{\cdot}0$ on the roof.

(3) Perforated tunnel with $F = 0$ and $\beta/P = 1{\cdot}0$ on the roof.

No new techniques were required for cases (1) and (3), but for cases (2) the boundary condition to be satisfied is

$$\partial\phi/\partial Z = -(P/\beta)\,(\partial\phi/\partial X + F\partial^2\phi/\partial X\partial Z). \tag{32}$$

The step by step method is exactly the same as that used for the perforated boundary and described in Section 5.2. Though the convergence requires a similar number of steps, considerably more numerical

work is required in evaluating the right hand side of equation (32).

Values of δ_0 and δ_1 are recorded in Table 4, and included in this table are analytical values taken from the curves in Figure 3 in Reference 7. In Figure 12 the distribution of δ is plotted for each of these three cases.

TABLE 4

	Resistance Network		Analytical
Case	δ_0	δ_1	δ_0
1	−0·09655	−·1268	−0·10
2	+·01752	+·1584	+0·018
3	+·00204	+·1356	+0·010

5.4. *Slots Covered with Perforations.*

Many slotted tunnels are being tested with the slots covered by perforations, and therefore a series of tests were carried out to determine the effect of the porous sheet covering slots on the interference parameters of slotted tunnels. One particular tunnel was studied with a single centrally placed slot on the centreline of the tunnel roof, the width of the slot was one eight of the breadth of the tunnel.

The equation to be satisfied on the open portion of the slot was

$$\partial\phi/\partial X + (\beta/P)(\partial\phi/\partial Z) = 0\,, \tag{13}$$

with β/P taken as 0, 0·3, 0·7, 1·0, ∞, where $\beta/P = 0$ is equivalent to a tunnel with a slot without any perforations and $\beta/P = \infty$ is equivalent to a totally closed tunnel.

The occurrence of a slot introduces a singularity at the edges of the slot. An automatic method of representing the singularity is possible by modifying the values of the resistance at the edge of the slot as described in Reference 8. Then the procedure for satisfying the porous condition is the same as for the perforated boundary, described in Section 5.2.

In Figure 14 the results for δ_0 and δ_1 are plotted against $(1+\beta/P)^{-1}$. Also the distribution of δ along the tunnel axis is recorded in Figure 13. These results indicate that the presence of the perforations change the interference pattern to be very close to the fully closed condition even with a low value of β/P.

6. *Conclusions.*

This Report has shown that the lift interference effects in steady flow, in wind tunnels with various boundaries can be analysed thoroughly using a resistance-network analogue computer to solve the finite-difference equation. Detailed results have been presented for a series of typical tunnels and there is no reason why any wind tunnel with slotted or perforated boundaries cannot be analysed.

As an alternative to using a resistance network an attempt is being made to programme the work for a digital computer. This becomes possible since a new numerical technique called Dynamic Relaxation[10] can be used as an alternative to the analogue solution of the Laplace equation in three dimensions. Preparatory work on the topic is showing promise.

Generally the accuracy of the results from the analogue computer have been adequate. Greater precision will be possible from a digital solution but there will still be the inherent error of the finite difference approach. In the particular case of the evaluation of δ_0' the limited accuracy is primarily due to the finite difference error. Because the practical size of the resistance network and the available time on a

digital computer are restricted, any appreciable reduction in the finite-difference mesh spacing is not, at present, possible.

Future work on the analogue computer will include an investigation into oscillatory, incompressible flow. Equations describing this flow have real and imaginary parts which will satisfy the Laplace equation. Separate three-dimensional resistance networks will be used for the real and imaginary parts of the velocity potential with interreacting boundary conditions.

7. *Acknowledgements.*

The study of wind-tunnel interference effects using an analogue computer, described in this report, is part of a contract with the Ministry of Aviation.

The particular investigations carried out were suggested by Mr. Garner of the National Physical Laboratory, and his constant interest during the course of the work is gratefully acknowledged.

LIST OF SYMBOLS

b	Tunnel breadth
C_L	Lift coefficient
d	Interval between mesh points
F	Non-dimensional slot parameter, $2K/h$
G, G'	Scaling factors
h	Tunnel height
K	Geometric slot parameter in equation (7) of Ref. 1
M	Mach number of undisturbed stream
n	Outward normal distance from tunnel boundary
P	Porosity parameter
R, R'	Resistances
S	Planform area
t	Time
U	Undisturbed stream velocity
U_0, V	Voltages
x,y,z	Co-ordinates
X,Y,Z	Transformed co-ordinates in equation (3)
β	$(1-M^2)^{\frac{1}{2}}$
δ	Distribution of interference upwash along the axis of the tunnel (equation 16)
δ_0	Lift-interference parameter in equation (15)
δ_1	Lift-interference parameter associated with streamline curvature in equation (18)
δ_0'	Interference parameter in equation (17)
ϕ	Perturbation velocity potential
ϕ_i	Interference velocity potential
ϕ_m	ϕ for model in unconstrained flow
θ	Angle

REFERENCES

No.	*Author(s)*	*Title, etc.*
1	K. R. Rushton	Studies of slotted-wall interference using an electrical analogue. A.R.C. R. & M. 3452. June 1965.
2	D. D. Davis and D. Moore . .	Analytical study of blockage and lift-interference corrections for slotted tunnels obtained by the substitution of an equivalent homogeneous boundary for discrete slots. NACA R.M. L53E07b (NACA/T1B/3792). 1953.
3	B. S. Baldwin, J. B. Turner and E. D. Knechtel . .	Wall interference in wind tunnels with slotted and porous boundaries at subsonic speeds. NACA Tech. Note 3176. 1954.
4	Sune B. Berndt	Wind tunnel interference due to lift for delta wings of small aspect ratio. KTH (Sweden) Aero TN 19. 1950.
5	P. F. Maeder, G. F. Anderson and J. B. Carroll	Experimental investigation of subsonic wall interference in rectangular slotted test sections. Brown Univ. Div. of Eng. Tech. Report. (Unpublished).
6	K. C. Wight	A review of slotted-wall wind-tunnel interference effects on oscillating models in subsonic and transonic flows. *J. Ry. aero. Soc.* Vol. 68, pp. 670–674. 1964.
7	D. R. Holder	Upwash interference on wings of finite span in a rectangular wind tunnel with closed side walls and porous-slotted floor and roof. A.R.C. R. & M. 3395, November 1963.
8	K. R. Rushton and R. Herbert	Special techniques required to represent practical groundwater flow systems on a resistance network. Dept. of Civ. Eng. Unit. of B'ham. Research Report. 1966.
9	H. C. Garner, A. W. Moore and K. C. Wight . .	The theory of interference effects on dynamic measurements in slotted-wall tunnels at subsonic speeds and comparisons with experiment. A.R.C. R. & M. 3500. September 1966.
10	J. R. H. Otter	Computations for prestressed concrete reactor pressure vessels using dynamic relaxation. *Nuclear Structural Engineering*, Vol. 1, pp. 61–75. 1965.

APPENDIX

Evaluation of δ_0'.

Since this project commenced the importance of an interference parameter, δ_0', has become apparent,[9] where,

$$\delta_0' = -\frac{1}{h}\int_{-\infty}^{0} \delta(X)\,dX \tag{A.1}$$

The determination of δ_0' involves integrating δ upstream to infinity and it is therefore desirable to know accurately the values of δ at planes far upstream. When the network was designed it was only thought necessary to continue far enough towards minus infinity to give good results of δ_0 and δ_1 at the wing. Hence there is some difficulty in evaluating δ_0' because of the grading of the network far upstream.

Since part of the integral is between minus infinity and the last plane represented by the resistance network, it is not sufficient to calculate δ_0' only from the area under the curve between this plane and the wing. For this reason the values of δ were fitted to the following function between the wing and minus infinity:

$$\delta = (A_0 + B_1 \sin\theta)\cos^2\theta \tag{A.2}$$

The coefficients A_0 and B_1 took different values for each mesh interval and also were arranged to satisfy both end values.

The closed tunnel was considered in detail. Initially analytical solutions of δ at the analogue mesh intervals were used to calculate δ_0' and the result obtained in this was very close to the analytical value of δ_0'. Thus, it was proved that this method of evaluating δ_0' is satisfactory. However, when the analogue results were substituted in the formula, there was poor agreement between this value of δ_0' and the analytical solution.

Since the poor result was due to the mesh spacing far upstream an alternative solution with a different mesh spacing was used. The length of the tunnel was extended to $X = -10$ and more mesh points were provided in the region far upstream.

A network of 5 x 5 x 10 was used, thus a coarser mesh spacing was adopted in the Y and Z directions and in the X direction near to the wing. Therefore inaccuracies in δ_0 and δ_1 occurred; δ_0 was nearly 10 per cent in error. However a comparison of the distribution of δ with the analytical solution of Figure 7 shows that with the new mesh spacing, the zero value of δ occurred at the correct position of X.

When these results were fitted into equation (A.2) a satisfactory value of δ_0' was obtained. The values are shown in Table A.1 and compared with analytical and previous analogue results.

TABLE A.1

	δ_0'	
	Closed tunnel	Open tunnel
Analytical solution	−0·0361	+0·0814
Original mesh spacing	−0·0179	+0·0807
New mesh spacing	−0·0372	

Further work is being carried out into the evaluation of δ_0' for porous and non-ideal slotted tunnels.

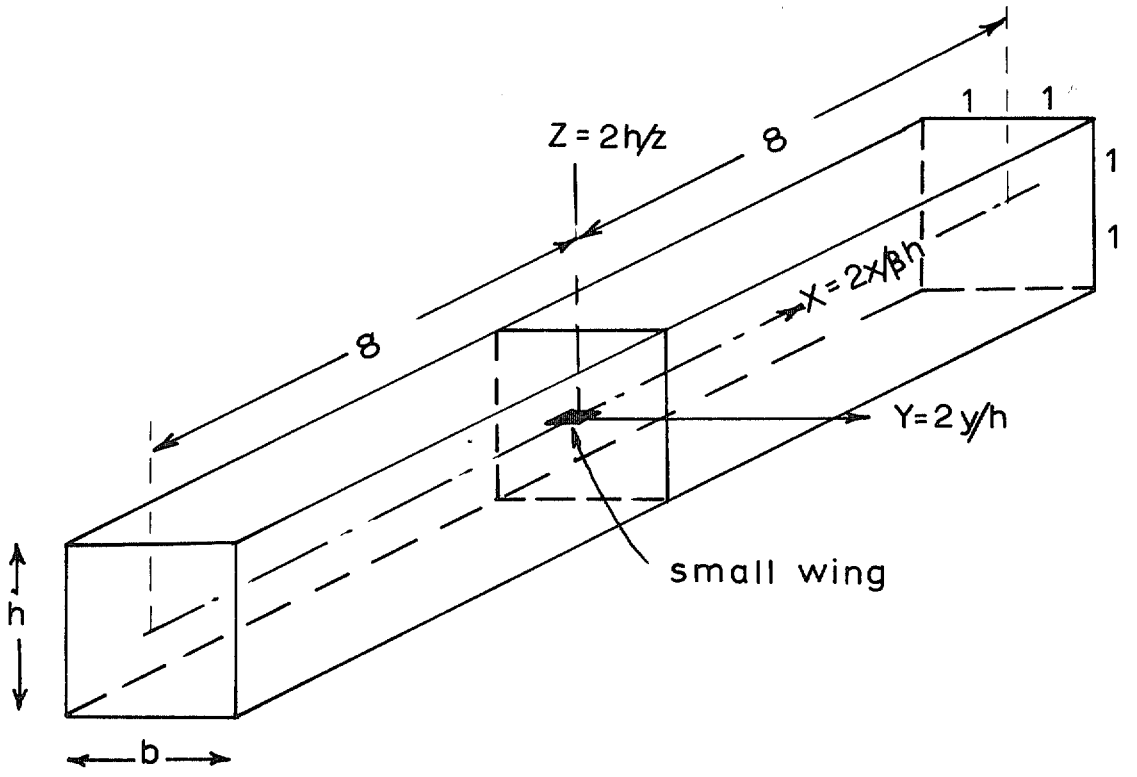

FIG. 1. Small wing in tunnel.

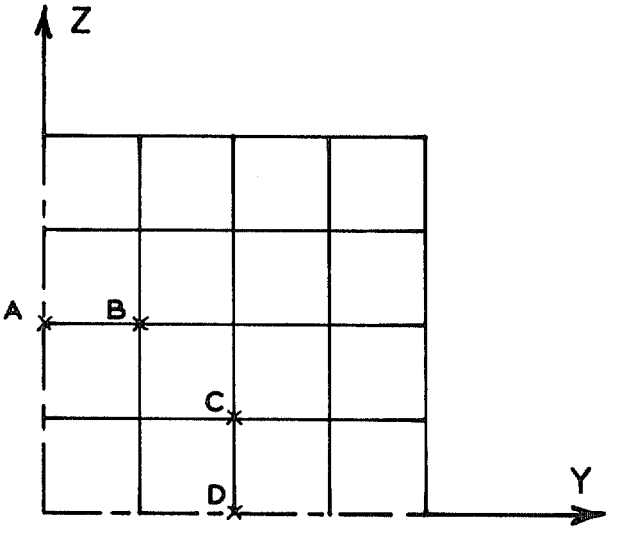

FIG. 2. Arc representing small wing.

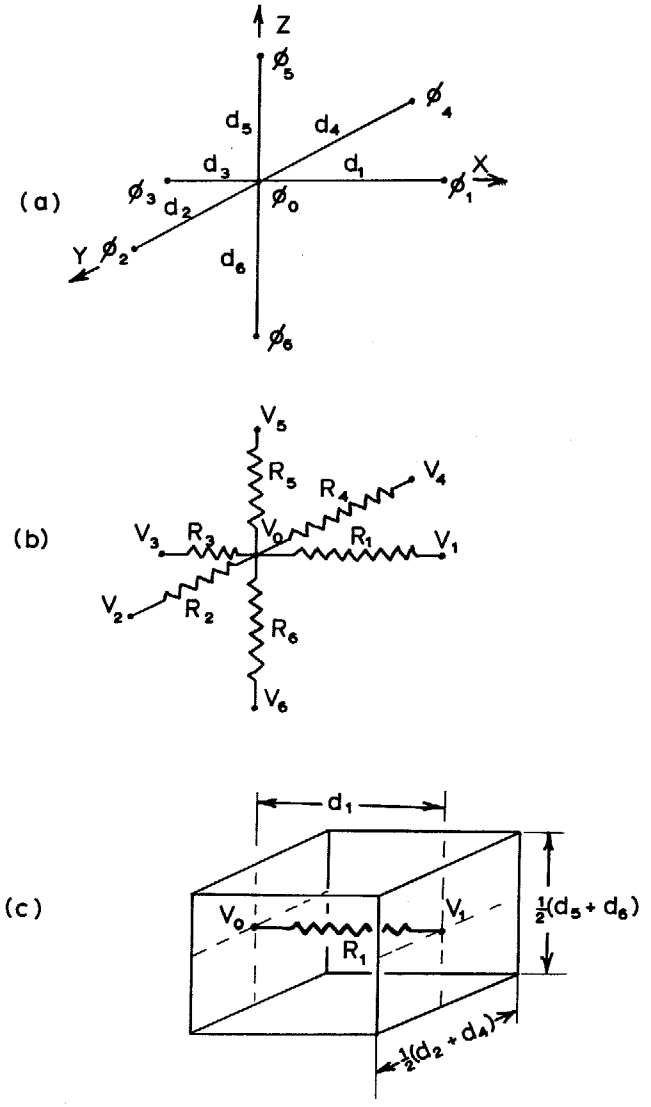

FIG. 3. Finite difference and resistor meshes.

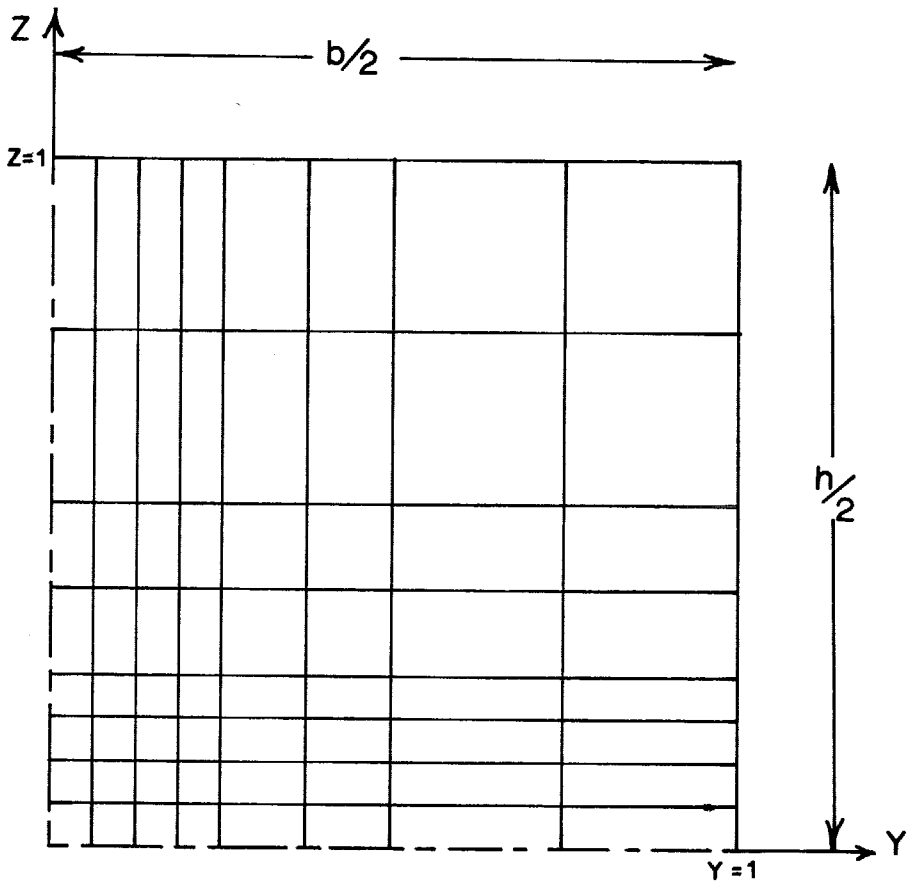

FIG. 4. Mesh spacing of square three-dimensional tunnel, for a plane X = constant.

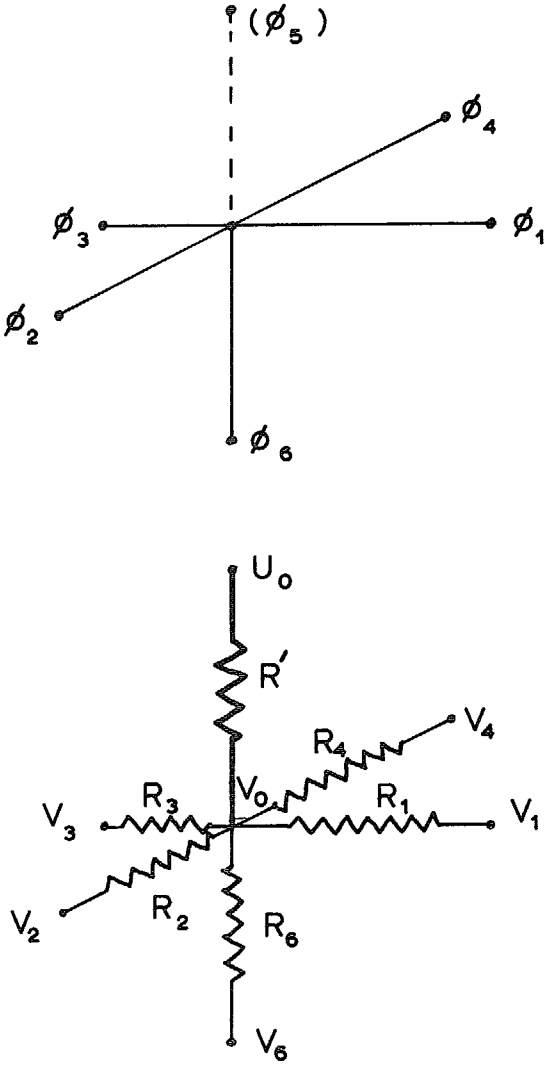

FIG. 5. Finite difference and resistor meshes for a specified slope.

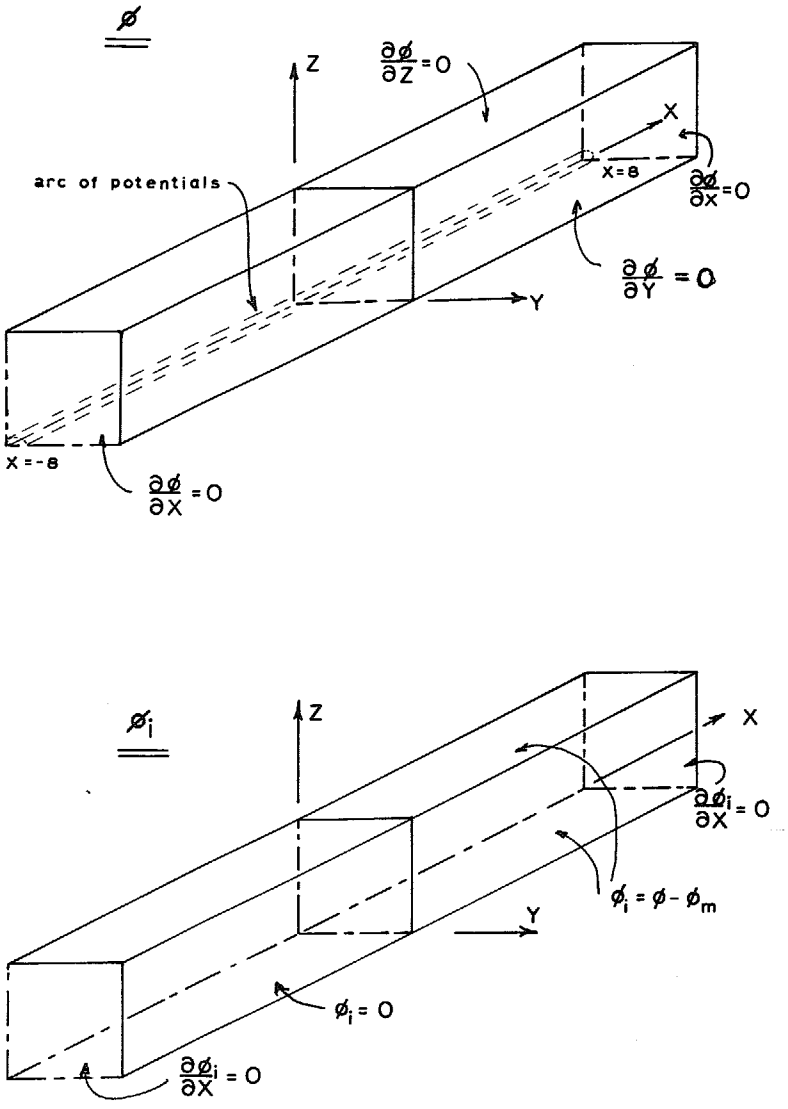

FIG. 6. Conditions applied on network for a closed tunnel.

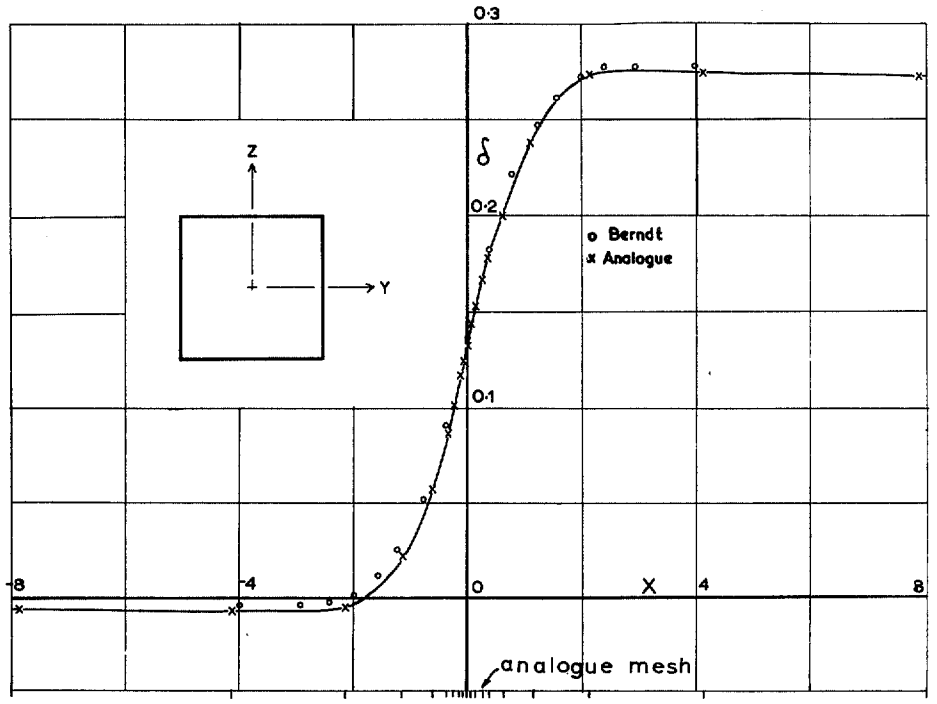

FIG. 7. Distribution of δ for a closed tunnel, comparison with Berndt's expression.

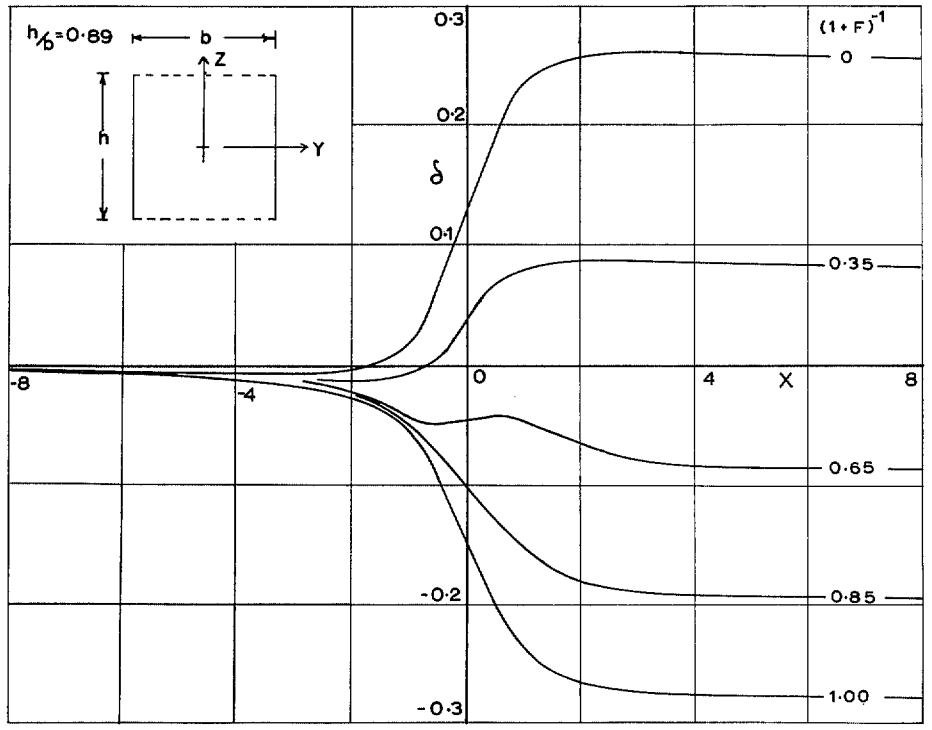

FIG. 8. Distribution of δ in a tunnel with $h/b = 0{\cdot}89$ with the roof and floor slotted.

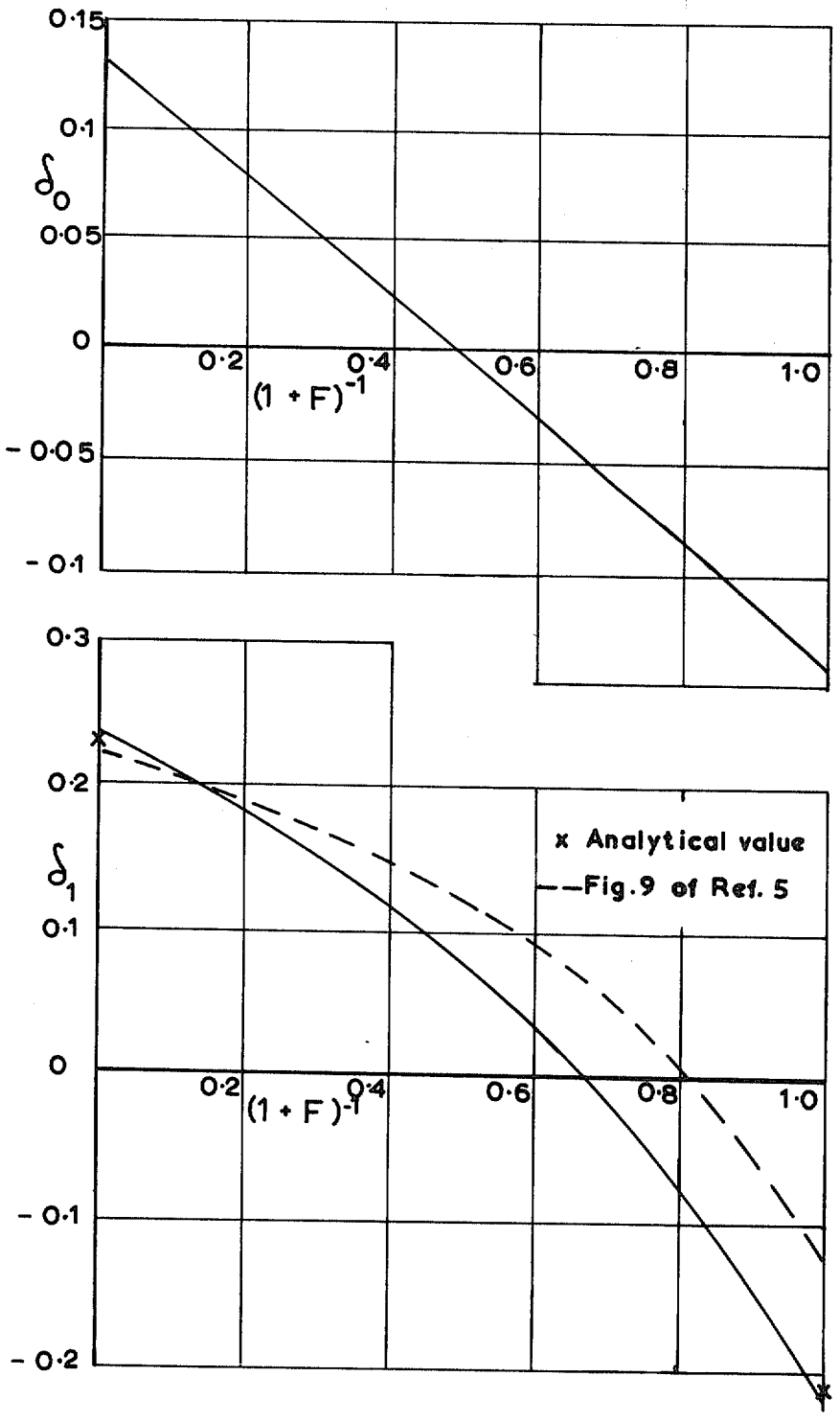

FIG. 9. Variation of δ_0 and δ_1 for ideal slotted tunnel.

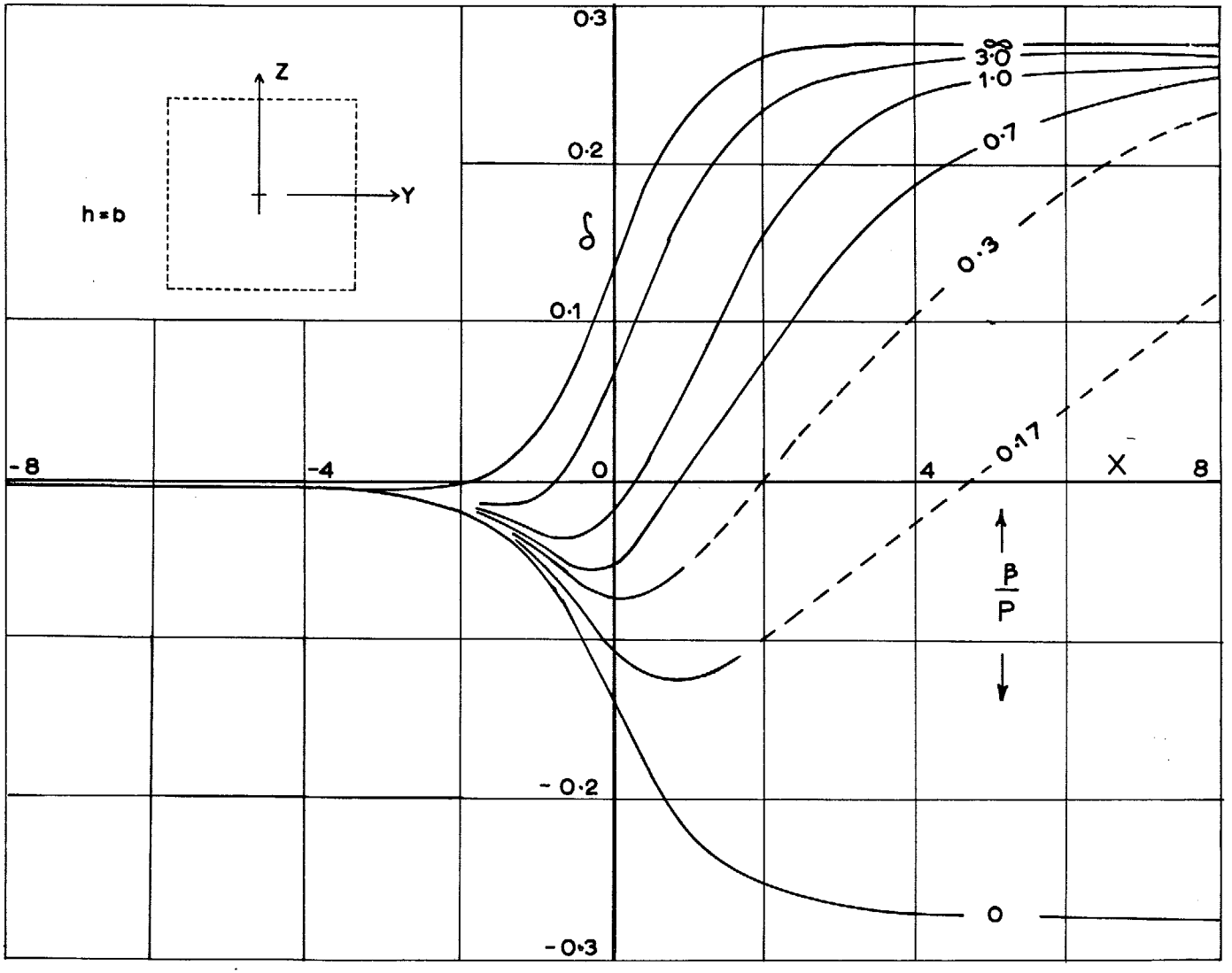

FIG. 10. Distribution of δ in a square tunnel with all walls perforated.

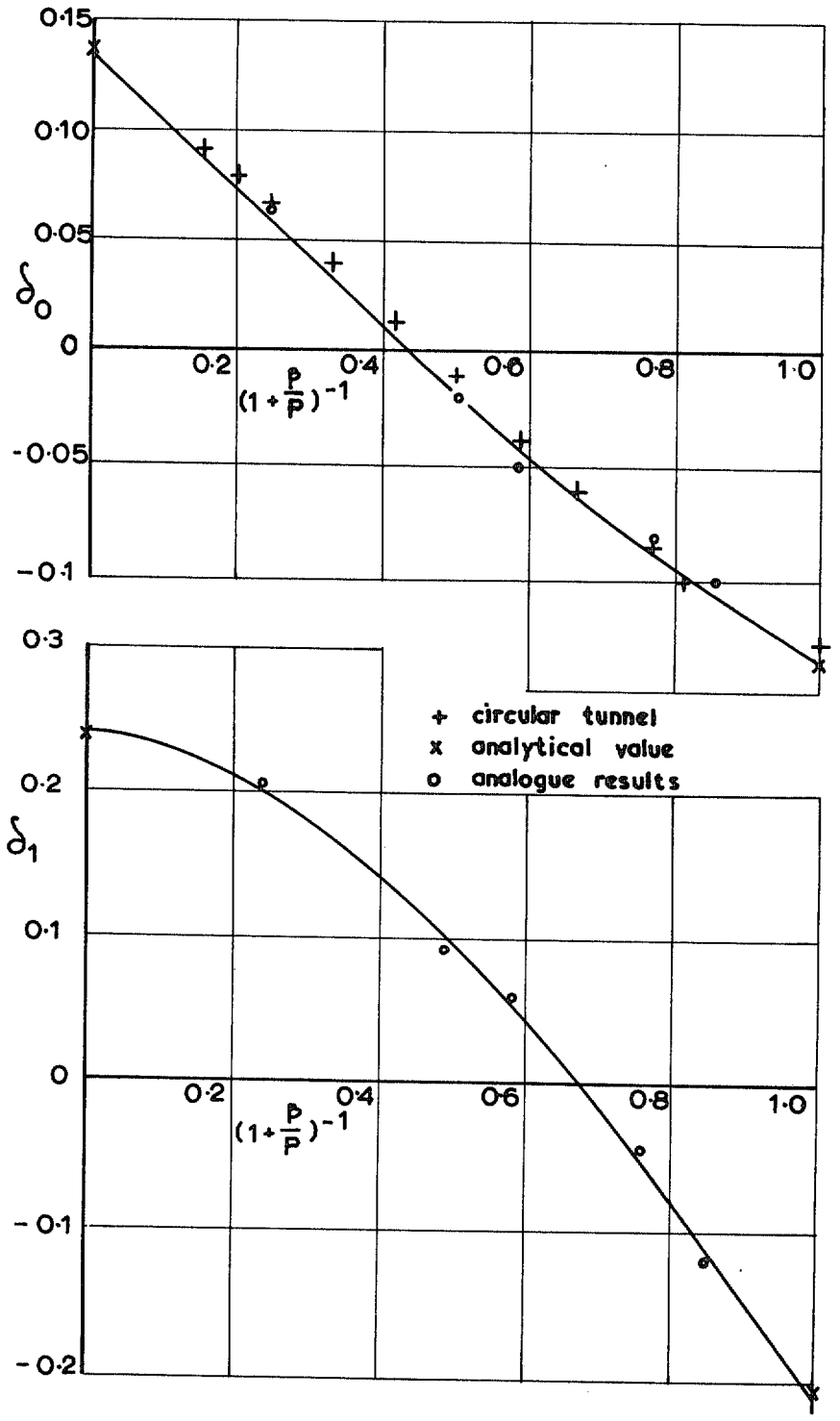

FIG. 11. Variation of δ_0 and δ_1 for tunnel with perforated roof and walls. + circular tunnel; × analytical value; o analogue results.

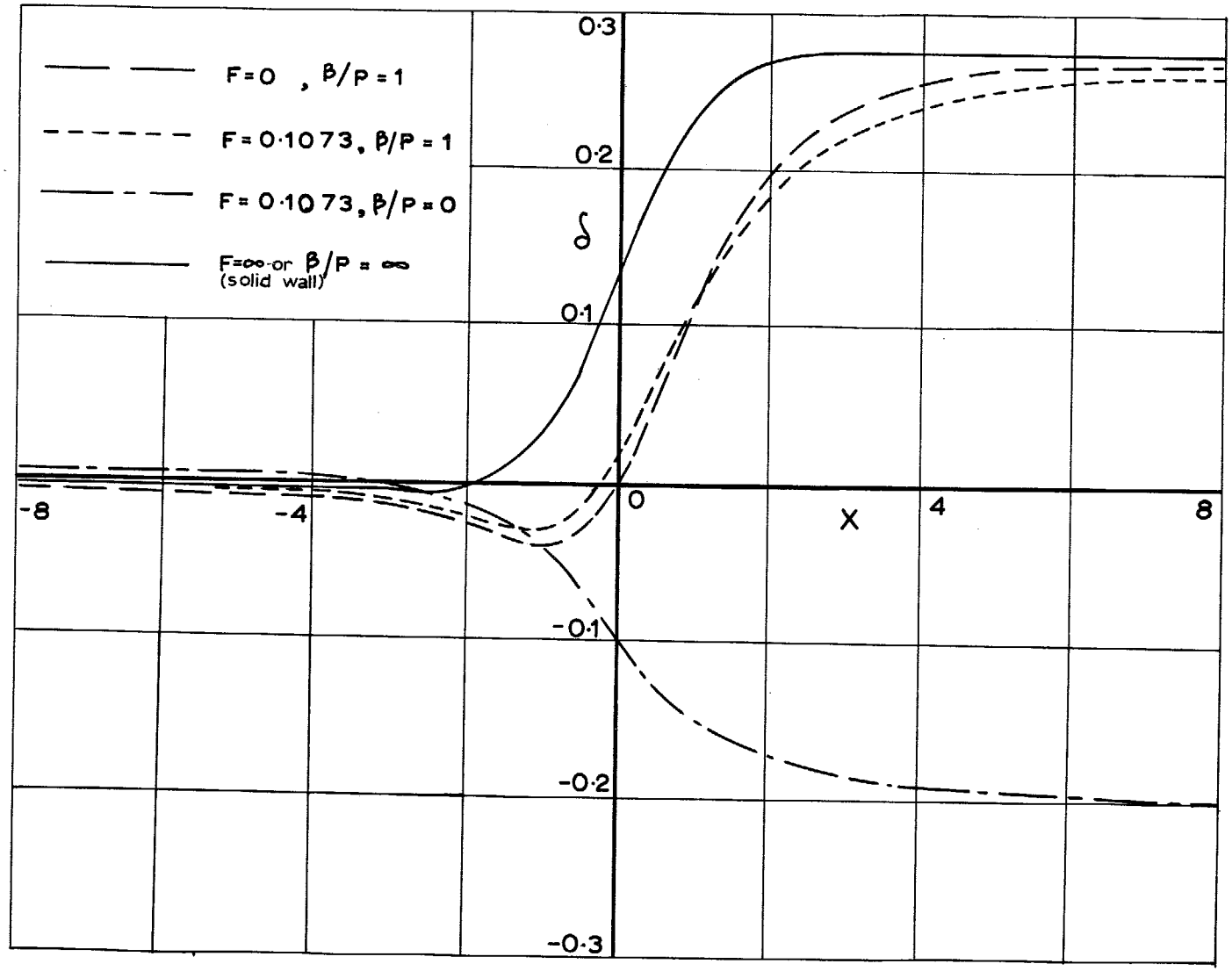

FIG. 12. Distribution of δ. Typical tunnel with various boundary conditions on roof but closed side walls.

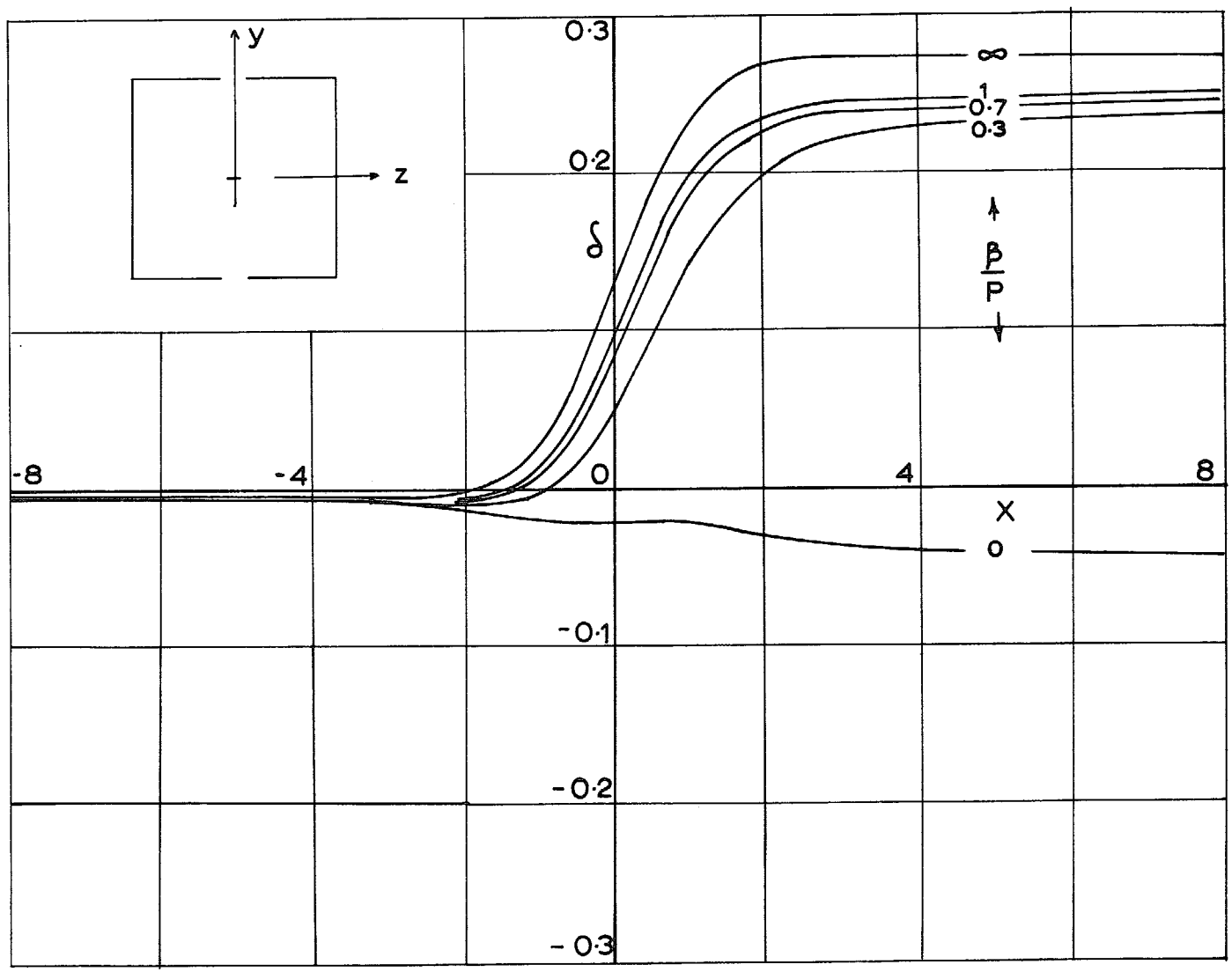

FIG. 13. Distribution of δ for square tunnel containing a single slot of width $\frac{1}{8}b$.

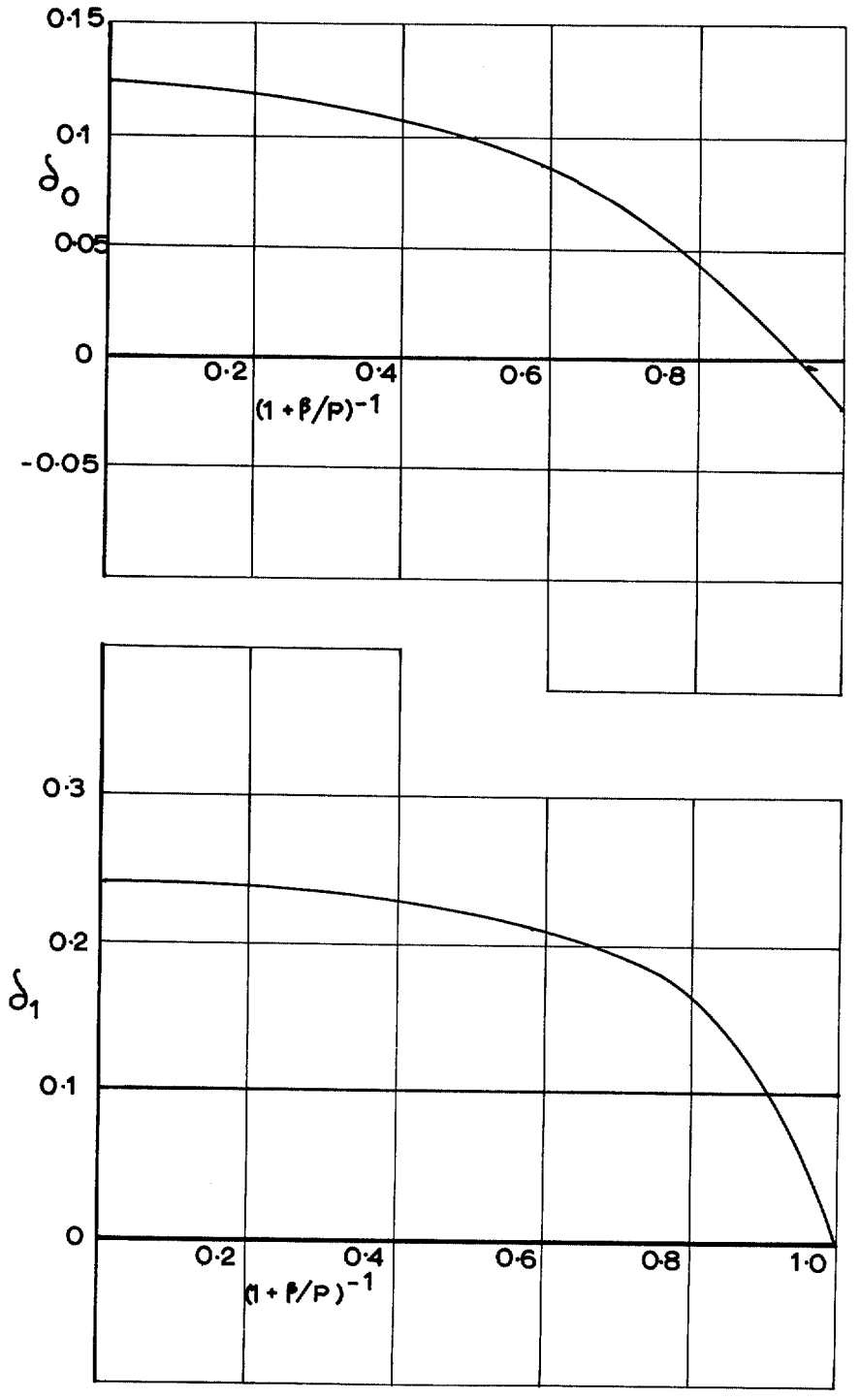

FIG. 14. Variation in δ_0 and δ_1 for tunnel with single slot covered by perforations.

Printed in Wales for Her Majesty's Stationery Office by Allens Printers (Wales) Limited.

Dd. 135646 K5

© *Crown copyright* 1969

Published by
HER MAJESTY'S STATIONERY OFFICE

To be purchased from
49 High Holborn, London W.C.1
13A Castle Street, Edinburgh 2
109 St. Mary Street, Cardiff CF1 1JW
Brazennose Street, Manchester M60 8AS
50 Fairfax Street, Bristol BS1 3DE
258 Broad Street, Birmingham 1
7 Linenhall Street, Belfast BT2 8AY
or through any bookseller

R. & M. No. 3567

S.O. Code No. 23-3567